68Ga-PSMA-HBED-CC Uptake in Cervical, Celiac, and Sacral Ganglia as an Important Pitfall in Prostate Cancer PET Imaging

Christoph Rischpler[1,2]*, Teresa I. Beck[3]*, Shozo Okamoto[1,4], Anna M. Schlitter[5], Karina Knorr[1], Markus Schwaiger[1], Jürgen Gschwend[6], Tobias Maurer[6,7], Philipp T. Meyer[3], and Matthias Eiber[1]

[1]Department of Nuclear Medicine, Klinikum Rechts der Isar, Technical University of Munich, Munich, Germany; [2]Department of Nuclear Medicine, University Hospital Essen, University of Duisburg-Essen, Essen, Germany; [3]Department of Nuclear Medicine, Medical Center–University of Freiburg, Faculty of Medicine, University of Freiburg, Freiburg, Germany; [4]Department of Nuclear Medicine, Hokkaido University Graduate School of Medicine, Sapporo, Japan; [5]Institute of Pathology, Technical University Munich, Munich, Germany; [6]Department of Urology, Klinikum Rechts der Isar, Technical University of Munich, Munich, Germany; and [7]Martini Klinik, University Medical Center Hamburg-Eppendorf, Hamburg, Germany

The study aims to investigate the presence of physiologic prostate-specific membrane antigen (68Ga-PSMA)-ligand uptake on PET in cervical, celiac, and sacral ganglia of the sympathetic trunk as a pitfall for lymph node metastases in prostate cancer imaging. **Methods:** Four hundred seven patients who underwent Glu-NH-CO-NH-Lys radiolabeled with 68Ga-gallium N,N-bis[2-hydroxy-5-(carboxyethyl) benzyl]ethylenediamine-N,N-diacetic acid (68Ga-PSMA-HBED-CC) PET (combined with a diagnostic CT) were retrospectively analyzed. The number of 68Ga-PSMA PET–positive cervical, celiac, and sacral ganglia was determined, and the configuration and SUV_{max} of each ganglion were measured. In addition, the configuration and SUV_{max} of adjacent lymph node metastases in the respective region (cervical, celiac, or sacral) were determined. **Results:** 68Ga-PSMA-ligand uptake above background was detected in 401 (98.5%) patients in any peripheral ganglia, in 369 (92%) patients in cervical ganglia, in 363 (89%) patients in celiac ganglia, and in 183 (46%) patients in sacral ganglia. The 68Ga-PSMA-ligand uptake was highest in celiac (mean SUV_{max}, 2.9 ± 0.8 vs. cervical mean SUV_{max}, 2.4 ± 0.6) and sacral (mean SUV_{max} 1.7 ± 0.5; both $P < 0.0001$) ganglia. Intraindividually there was a statistically significant but weak to moderate correlation between the 68Ga-PSMA-ligand uptake in cervical versus celiac ganglia ($R = 0.34$, $P < 0.0001$), cervical versus sacral ($R = 0.52$, $P < 0.0001$), and celiac versus sacral ($R = 0.16$, $P < 0.05$). The 68Ga-PSMA-ligand uptake was significantly more intense in adjacent lymph node metastases than the respective ganglia (cervical: 18.0 ± 16.2 vs. 2.4 ± 0.6, $P < 0.0001$; celiac: 13.5 ± 12.3 vs. 2.9 ± 0.8, $P < 0.0001$; sacral: 13.4 ± 11.6 vs. 1.7 ± 0.5, $P < 0.0001$). Furthermore, ganglia predominantly exhibit a band-shaped configuration (71.2%), followed by a teardrop (26.8%) and only rarely a nodular configuration (2.0%). Conversely, lymph node metastases are only rarely band-shaped (1.1%), but more often show teardrop (40.3%) or nodular appearance (58.6%) ($P < 0.00001$). **Conclusion:** 68Ga-PSMA-ligand uptake in ganglia along the sympathetic trunk as assessed by 68Ga-PSMA-HBED-CC PET represents an important pitfall in prostate cancer PET imaging. The 68Ga-PSMA-ligand uptake is higher in celiac ganglia than cervical or sacral ganglia, and the level of 68Ga-PSMA-ligand uptake seems to be patient-related. For the differentiation between lymph node metastases and sympathetic ganglia, both intensity of 68Ga-PSMA-ligand uptake and exact localization and configuration of the respective lesion should be examined carefully.

Key Words: oncology: GU; PET; PET/CT; 68Ga-PSMA; PET; 68Ga-PSMA expression; pitfall; prostate cancer

The prostate-specific membrane antigen (68Ga-PSMA) is a membrane-bound enzyme, which is highly expressed on prostate cancer cells and its metastases (1). It is also named glutamate carboxypeptidase II based on its enzymatic function. 68Ga-PSMA-targeted imaging using PET radiotracers, such as Glu-NH-CO-NH-Lys radiolabeled with 68Ga-gallium N,N-bis[2-hydroxy-5-(carboxyethyl) benzyl]ethylenediamine-N,N-diacetic acid (68Ga-PSMA-HBED-CC), has therefore experienced an increasing demand during the last few years (2). In some centers, 68Ga-PSMA PET imaging is now regarded as the method of reference for staging and restaging of patients with confirmed (high-risk) prostate cancer or in the case of biochemical recurrence; furthermore, even at low prostate-specific antigen levels and for small lymph node metastases, 68Ga-PSMA PET imaging offers a high sensitivity (2–5).

However, high 68Ga-PSMA expression has also been described in malignant lesions not related to the prostate (e.g., renal cell carcinoma, bronchial carcinoma, glioblastoma), in benign tissues (e.g., renal tubules, duodenum, colon), and in benign lesions such as schwannomas, osteophytes, thyroid adenomas or vertebral and subcutaneous hemangiomas (1,6–14). The ganglia of the sympathetic trunk are another tissue in which an increased 68Ga-PSMA expression has been reported (15,16). Histologic studies have found that the glutamate carboxypeptidase II is highly expressed on nonmyelinating Schwann cells in ganglia of the sympathetic nervous system. This potentially explains 68Ga-PSMA-ligand uptake in various parts of the sympathetic nervous system (17).
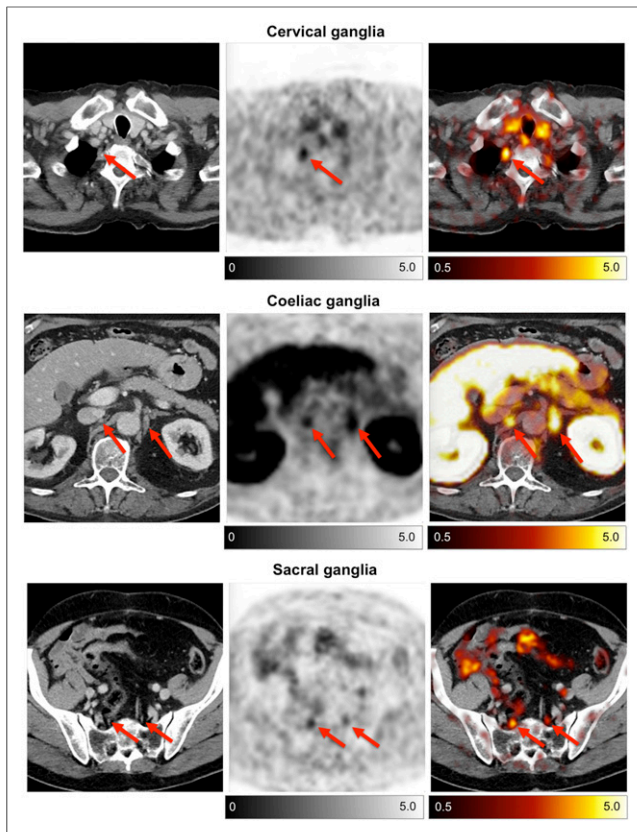
FIGURE 1. 68Ga-PSMA-HBED-CC uptake of cervical, celiac, and sacral ganglia. (Left) Diagnostic, contrast-enhanced CT. (Middle) 68Ga-PSMA-HBED-CC PET. (Right) Overlay of 68Ga-PSMA-HBED-CC PET and CT. Red arrows indicate ganglia at respective location.

As the sympathetic trunk runs along the vertebra, sympathetic ganglia can easily be confused with lymph node metastases that are often found near particularly to cervical, celiac, or sacral ganglia. Consequently, 68Ga-PSMA-ligand uptake in such ganglia is a potential source of misdiagnosis, which may even result directly in change of therapy regimen and therefore represents an important pitfall. The aim of this retrospective analysis was to give a detailed description of the incidence and imaging pattern in 68Ga-PSMA-HBED-CC PET/CT of cervical, celiac, and sacral ganglia to facilitate the discrimination from prostate cancer–related lymph node metastases.

MATERIALS AND METHODS

Patient Population, Radiotracer Synthesis, and Imaging Protocol

Four hundred seven patients from 2 centers (Technical University Munich and University of Freiburg) who underwent 68Ga-PSMA-HBED-CC PET/CT between October 2012 and August 2015 were randomly selected and analyzed. Only studies with a diagnostic CT were chosen to allow for detailed anatomic description of the configuration of ganglia and lymph node metastases.

The retrospective study was approved by the Ethics Committee of the Technical University Munich (permit 5665/13), and written informed consent was obtained from all patients for the purpose of anonymized evaluation and publication of their data. All reported investigations were conducted in accordance with the Helsinki Declaration and with national regulations.

PET/CT scans were obtained on a Siemens Biograph mCT (Siemens Healthcare) or a 64-slice GEMINI TF PET/CT (Philips Healthcare). Radiotracer synthesis was performed as previously described (3) and injected via an intravenous bolus (167 ± 28 MBq; range, 120–240 MBq). PET/CT acquisition was started 56 ± 8 min (range, 32–85 min) after tracer injection. The diagnostic CT scan was acquired after patients received oral contrast and in portal venous phase. Subsequently, the PET scan was acquired in 3-dimensional mode with an acquisition time of 3–4 min per bed position (Munich) or with 2 min per bed position, whole-body protocol with 50% overlap (Freiburg). Correction of emission data for randoms, dead time, scatter, and attenuation was performed. Iterative reconstruction of PET data by an ordered-subsets expectation maximization algorithm (4 iterations, 8 subsets) followed by a postreconstruction smoothing gaussian filter (5 mm in full width at one-half maximum) was performed (Munich), or PET list-mode data were reconstructed using a lines-of-response–based ordered-subsets algorithm with time-of-flight information in a $2 \times 2 \times 2$ mm voxel matrix (BLOB-OS-TF, 3 iterations, 33 subsets, relaxation parameter l = 0.35, no additional smoothing) (Freiburg).

Image Analysis

Images were analyzed by 2 experienced nuclear medicine physicians (4 and 12 y of training). PET and CT images were analyzed side by side and the number, location (left/right, cervical/celiac/sacral), 68Ga-PSMA-ligand uptake intensity (SUV$_{max}$ normalized to body weight and visual intensity ranging from 0 to 3 [faint/mild/moderate/intense uptake]; Fig. 1), and configuration (band, teardrop, or nodular shape; Fig. 2) of 68Ga-PSMA-positive sympathetic ganglia were assessed. Main criteria for ganglia were focal 68Ga-PSMA-ligand uptake that projected onto a structure with typical location for sympathetic ganglia. In a second step, the same parameters for definite lymph node metastases near the respective ganglia were determined, to investigate potential criteria for differentiation.

Histology

From patients who had an extensive surgery of the pelvis, sacral ganglia were obtained and stained for 68Ga-PSMA expression as previously described (18).

Statistics

Results are either demonstrated as frequencies (%) or as mean ± SD. P values less than 0.05 were considered statistically significant. For comparison of unmatched, continuous variables, the 2-tailed unpaired Student t test was used. The χ^2 test was applied to compare nominal variables. Matched continuous variables were compared using the 2-tailed paired Student t test. The association between continuous variables was investigated using the Pearson correlation coefficient. For statistical analyses MedCalc (version 17.4; MedCalc Software) for Windows (Microsoft) and SPSS Statistics for Windows (version 22.0; IBM Corp Released 2013; IBM Corp.) were used.
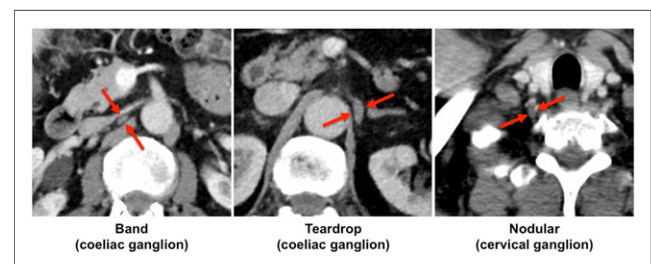

FIGURE 2. Overview of different anatomic configurations of ganglia. Red arrows indicate ganglia at respective location.

RESULTS

Prevalence and Semiquantitative 68Ga-PSMA-Ligand Uptake of Sympathetic Ganglia

On a per-patient basis, 68Ga-PSMA-ligand uptake in any peripheral sympathetic ganglia was detected in 98.5% (401/407 patients). Grouped by anatomy, local positive 68Ga-PSMA-ligand uptake was found at a frequency of 91.8% (369/402 patients), 89.4% (363/406 patients), and 45.5% (183/402 patients) in cervical, celiac, and sacral
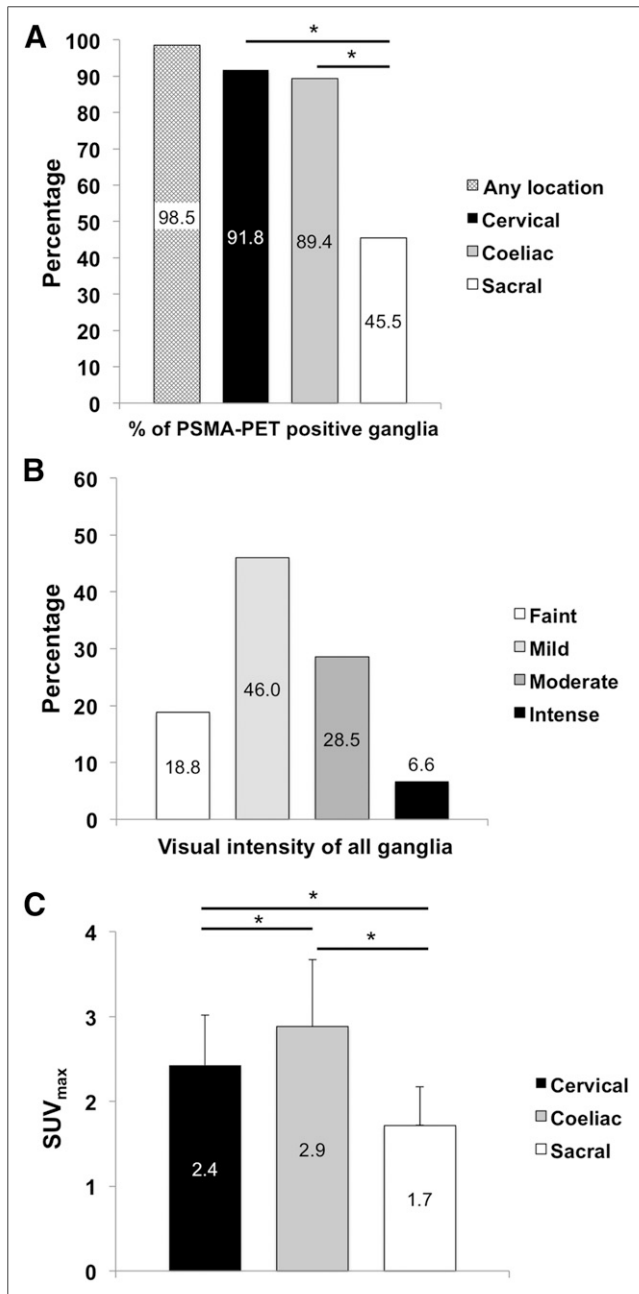

FIGURE 3. Number and uptake intensity of 68Ga-PSMA-HBED-CC–positive ganglia. (A) Frequencies (on per-patient-basis) of 68Ga-PSMA-HBED-CC uptake in any, celiac, cervical, and sacral ganglia. (B) Distribution of visual uptake intensities of sympathetic ganglia. (C) Quantitative comparison of 68Ga-PSMA-HBED-CC uptake (SUV$_{max}$) in sympathetic ganglia. *Significant differences.
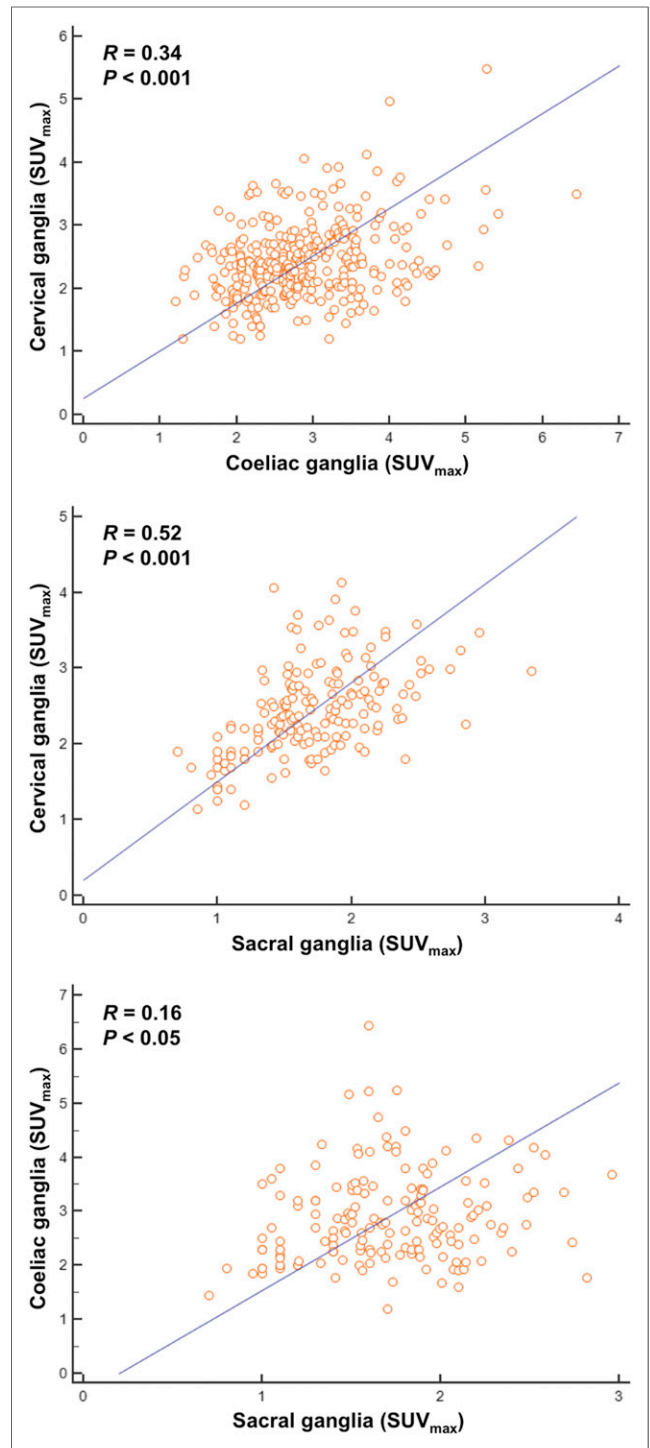

FIGURE 4. Intrapatient correlation of 68Ga-PSMA-HBED-CC uptake in cervical (top), celiac (middle), and sacral (bottom) ganglia, respectively.

ganglia, respectively (Fig. 3A). The lower rate of 68Ga-PSMA-positive sacral than cervical and celiac ganglia was highly statistically significant. Notably, because of adjacent bone or lymph node metastases 68Ga-PSMA-ligand uptake in cervical, celiac, and sacral ganglia could not be evaluated in 5, 1, and 5 patients, respectively.

^{68}Ga-PSMA-ligand uptake in ganglia was mostly rated as "mild" or "moderate" and less often as "faint" or "intense" (Fig. 3B). Absolute ^{68}Ga-PSMA-ligand uptake was highest in celiac ganglia followed by cervical and sacral ganglia (celiac mean SUV$_{max}$, 2.9 ± 0.8; cervical mean SUV$_{max}$, 2.4 ± 0.6; sacral mean SUV$_{max}$, 1.7 ± 0.5; $P < 0.0001$ for all pairs) (Fig. 3C). There was a weak to moderate but significant correlation of ^{68}Ga-PSMA-ligand uptake between different ganglia within a patient (cervical vs. celiac [$n = 327$]: $r = 0.34$, $P < 0.0001$; cervical vs. sacral [$n = 169$]: $r = 0.52$, $P < 0.0001$; and celiac vs. sacral [$n = 163$]: $r = 0.16$, $P < 0.05$) (Fig. 4).

Comparison of Anatomic Configuration and Quantitative Uptake Pattern of Ganglia and Adjacent Lymph Node Metastases

On a per-patient basis, ^{68}Ga-PSMA-ligand–positive lymph node metastases in any location (i.e., cervical, celiac, or sacral) were detected in 34.1% (139/407 patients). Grouped by anatomy, local ^{68}Ga-PSMA-ligand–positive lymph nodes metastases were found at a frequency of 7.4% (30/407 patients), 12.5% (51/407 patients), and 27.5% (112/407 patients) near the typical location of cervical, celiac, and sacral ganglia, respectively. Frequencies between the occurrence of ^{68}Ga-PSMA-positive ganglia and lymph node metastases were different for any and each separate location ($P < 0.0001$). ^{68}Ga-PSMA-ligand uptake in lymph node metastases was significantly higher than in ganglia for cervical, celiac, and sacral locations (cervical [$n = 28$]: 18.3 ± 16.8 vs. 2.6 ± 0.7, $P < 0.0001$; celiac [$n = 44$]: 12.0 ± 10.6 vs. 2.9 ± 0.8, $P < 0.0001$; sacral [$n = 54$]: 14.6 ± 12.8 vs. 1.8 ± 0.4, $P < 0.0001$) (Fig. 5B).

Furthermore, substantial differences in the anatomic configuration of ganglia compared with (adjacent) lymph node metastases were found. Ganglia predominantly exhibited a band-shaped configuration (all ganglia: 71.2%; cervical: 57.5%; celiac: 81.3%; sacral: 81.1%), followed by a teardrop (all ganglia: 26.8%; cervical: 38.5%; celiac: 18.1%; sacral: 18.5%) and only rarely a nodular configuration (all ganglia: 2.0%; cervical: 4.0%; celiac: 0.6%; sacral: 0.4%). Conversely, lymph node metastases were only rarely band-shaped (all lymph node metastases: 1.1%; cervical: 1.7%; celiac: 1.7%; sacral: 0.5%) but more often showed teardrop (all lymph node metastases: 40.3%; cervical: 39.7%; celiac: 47.9%; sacral: 35.9%) or nodular appearance (all lymph node metastases: 58.6%; cervical: 58.6%; celiac: 50.4%; sacral: 63.6%) ($P < 0.00001$; Fig. 6).

In a small number of patients with extensive surgery, immunhistochemical staining for ^{68}Ga-PSMA expression in sympathetic ganglia was performed (Fig. 5A). ^{68}Ga-PSMA expression was visually clearly more intense in lymph node metastases in comparison to sympathetic ganglia.

DISCUSSION

Recently, ^{68}Ga-PSMA PET has grown rapidly, and more and more centers worldwide offer this promising imaging modality for staging and restaging of prostate cancer (2). With the increasing number of scanned patients and the growing distribution of ^{68}Ga-PSMA PET, nuclear medicine physicians and radiologists need to become familiar with pearls and pitfalls of this imaging modality (19). Several malignancies and also benign structures that exhibit an elevated ^{68}Ga-PSMA expression have already been described (1,6–14).

In this retrospective analysis, we investigated in detail the ^{68}Ga-PSMA-ligand uptake in ganglia of the sympathetic trunk using ^{68}Ga-PSMA-HBED-CC PET/CT and compared these findings and parameters with the most often confounding structure, namely adjacent lymph node metastases. To the best of our knowledge, our study represents the largest cohort analyzing ^{68}Ga-PSMA-ligand uptake using ^{68}Ga-PSMA-HBED-CC in ganglia so far. Furthermore, we investigated the ^{68}Ga-PSMA-ligand uptake patterns at different locations (cervical, celiac, and sacral) and found that the intensity of ^{68}Ga-PSMA-ligand uptake is a patient-related phenomenon. Last, as a novelty we performed a systematic comparison of the different sympathetic ganglia and adjacent lymph node metastases and demonstrated that ^{68}Ga-PSMA-ligand uptake is higher in lymph node metastases and that lymph node metastases show a clearly different configuration in comparison to sympathetic ganglia.

For an inexperienced reader, ^{68}Ga-PSMA-ligand uptake in cervical, celiac, or sacral ganglia may be misinterpreted as pathologic ^{68}Ga-PSMA expression in soft-tissue structures, particularly lymph node metastases, which in turn may result in debilitating, therapeutic consequences for the patient. For instance, misinterpretation of ganglia as distant lymph node metastases in the case of primary staging may result in systemic medical (antihormonal therapy combined with chemotherapy) versus curative surgical treatment.

In general, the number, location, and appearance of ganglia described in the
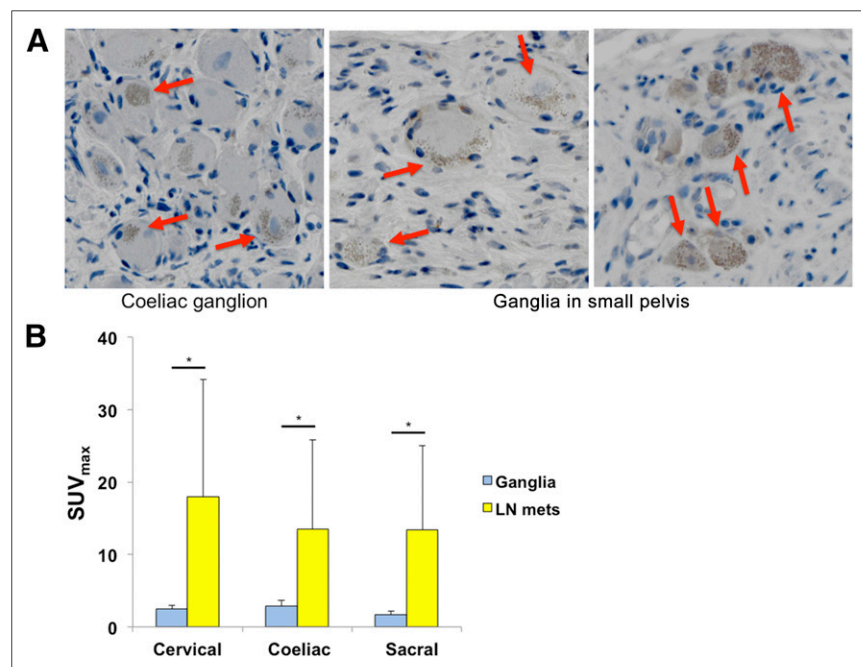

FIGURE 5. ^{68}Ga-PSMA expression and ^{68}Ga-PSMA-HBED-CC uptake in sympathetic ganglia and lymph node metastases. (A) Examples of immunohistochemical staining for ^{68}Ga-PSMA in ganglia. (B) Comparison of ^{68}Ga-PSMA-HBED-CC uptake in ganglia and adjacent lymph node metastases. Red arrows indicate ^{68}Ga-PSMA expression in ganglia. *$P < 0.0001$. Mets = metastases.
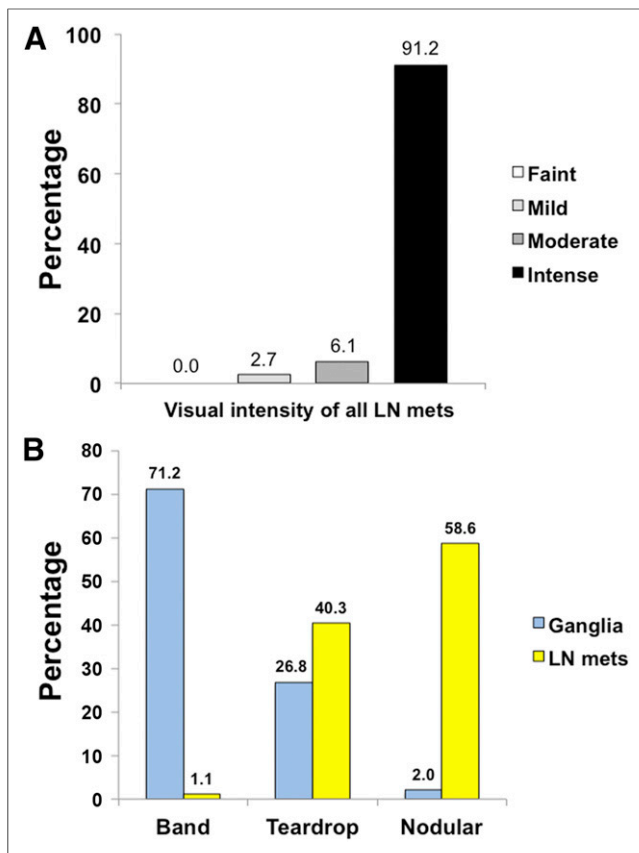
FIGURE 6. ^{68}Ga-PSMA-HBED-CC uptake of lymph node metastases and configuration of sympathetic ganglia and adjacent lymph node metastases. (A) Distribution of visual uptake intensities of lymph node metastases adjacent to sympathetic ganglia. (B) Configuration of sympathetic ganglia and adjacent lymph node metastases. LN = lymph node; mets = metastases.

present study is in line with previously published reports, in which ^{68}Ga-PSMA-ligand PET/CT or CT was used (15,20,21). More specifically, we were able to demonstrate that ^{68}Ga-PSMA-ligand uptake assessed by ^{68}Ga-PSMA-HBED-CC PET is highest in celiac ganglia, followed by cervical and sacral ganglia. Despite this fact, ^{68}Ga-PSMA PET–positive cervical and celiac ganglia were found at a similar frequency, most likely because background surrounding cervical ganglia is lower than in the celiac region. Notably, however, lymph node metastases in the cervical region are rather untypical; challenges to discriminate ganglia from lymph node metastases occur only very rarely. Furthermore, we showed that the ^{68}Ga-PSMA expression in ganglia of the sympathetic trunk is a patient-related phenomenon—that is, if a patient exhibits a high ^{68}Ga-PSMA-ligand uptake in one ganglia it is likely that the other ganglia also show an increased ^{68}Ga-PSMA expression—a finding that may help in the differentiation of ^{68}Ga-PSMA-ligand uptake in ganglia versus ^{68}Ga-PSMA-ligand uptake in adjacent lymph node metastases. The frequency reported in our analysis is slightly different than that in a recent publication reporting on peripheral ganglia seen on ^{18}F-DCFPyL PET/CT imaging (22). One might expect higher numbers for ^{68}Ga-PSMA-ligand PET–positive ganglia when using ^{18}F-labeled compounds (the lower positron range of ^{18}F may lead to a higher local circumscribed uptake). Comparison with current data in the literature does not back this hypothesis so far. However, differences between [18]F-

and ^{68}Ga-labeled ^{68}Ga-PSMA agents regarding affinity, internalization, and retention as well as local imaging techniques (e.g., injected dose, time between injection and imaging, emission time) might explain these variations. In addition, different scanner types, especially the emergence of digital PET techniques, might have substantial impact. So far, however, no studies directly comparing different PET scanners regarding ^{68}Ga-PSMA-ligand PET positivity of ganglia are available. Nevertheless, in principle, our results confirm that ^{68}Ga-PSMA-ligand uptake in sympathetic ganglia is a frequent observation also when using ^{68}Ga-PSMA-HBED-CC PET imaging.

In addition to the aforementioned recent publication, we also investigated and compared quantitative uptake as well as anatomic configuration of these ganglia compared with adjacent lymph node metastases. We demonstrated that the intensity of ^{68}Ga-PSMA-ligand uptake in lymph node metastases is significantly higher than in sympathetic ganglia. This is not unexpected given the usual high ^{68}Ga-PSMA expression of prostate cancer and its metastases compared with neurogenic tissue. In addition, the anatomic configuration assessed by CT is an important parameter, which may help in the differentiation of these 2 structures, because ganglia are more often band- and teardrop-shaped as opposed to lymph node metastases presenting with a nodular configuration. However, in the case of a ^{68}Ga-PSMA-ligand–positive teardrop-shaped structure the reader should not only rely on configuration but also consider additional features such as exact localization and intensity of radiotracer uptake. Nevertheless, we are convinced that both factors—configuration and intensity of ^{68}Ga-PSMA-ligand uptake—might aid the clinician in discriminating ganglia from adjacent lymph node metastases with relative high certainty. Notably, because size is not a reliable criterion to identify lymph node metastases (demonstrated by various studies using ^{68}Ga-PSMA-ligand PET (4)), the size of lymph nodes and ganglia were not assessed in our study.

This study has some limitations. The definition of ganglia and lymph node metastasis was based on characteristic imaging features only, such as typical anatomic location. However, because for ethical and practical reasons biopsies are only rarely obtained in metastatic prostate cancer, no histologic validation was possible. Nevertheless, we present immunohistochemical slices demonstrating ^{68}Ga-PSMA positivity of sympathetic ganglia, and there is accumulating evidence that false-positive findings in ^{68}Ga-PSMA PET is very low (23,24). In addition, on the basis of thorough review and experience of our readers, this approach seems reasonable. Finally, our study is of retrospective nature and only included patients who underwent a diagnostic CT within the hybrid PET/CT examination.

CONCLUSION

^{68}Ga-PSMA-ligand uptake in sympathetic ganglia is a very common and important pitfall using ^{68}Ga-PSMA-HBED-CC. However, on the basis of different anatomic configuration and uptake characteristics (intensity and intraindividual correlation of uptake), differentiation from possible adjacent lymph node metastases should be easily accomplishable.

DISCLOSURE

No potential conflict of interest relevant to this article was reported.

REFERENCES

1. Silver DA, Pellicer I, Fair WR, Heston WD, Cordon-Cardo C. Prostate-specific membrane antigen expression in normal and malignant human tissues. *Clin Cancer Res.* 1997;3:81–85.
2. Maurer T, Eiber M, Schwaiger M, Gschwend JE. Current use of PSMA-PET in prostate cancer management. *Nat Rev Urol.* 2016;13:226–235.
3. Eiber M, Maurer T, Souvatzoglou M, et al. Evaluation of hybrid ^{68}Ga-PSMA ligand PET/CT in 248 patients with biochemical recurrence after radical prostatectomy. *J Nucl Med.* 2015;56:668–674.
4. Giesel FL, Fiedler H, Stefanova M, et al. PSMA PET/CT with Glu-urea-Lys-(Ahx)-[[68]Ga(HBED-CC)] versus 3D CT volumetric lymph node assessment in recurrent prostate cancer. *Eur J Nucl Med Mol Imaging.* 2015;42:1794–1800.
5. Maurer T, Gschwend JE, Rauscher I, et al. Diagnostic efficacy of [68]gallium-PSMA positron emission tomography compared to conventional imaging for lymph node staging of 130 consecutive patients with intermediate to high risk prostate cancer. *J Urol.* 2016;195:1436–1443.
6. Rhee H, Ng KL, Tse BW, et al. Using prostate specific membrane antigen (PSMA) expression in clear cell renal cell carcinoma for imaging advanced disease. *Pathology.* 2016;48:613–616.
7. Pyka T, Weirich G, Einspieler I, et al. ^{68}Ga-PSMA-HBED-CC PET for differential diagnosis of suggestive lung lesions in patients with prostate cancer. *J Nucl Med.* 2016;57:367–371.
8. Chang SS, Reuter VE, Heston WD, Bander NH, Grauer LS, Gaudin PB. Five different anti-prostate-specific membrane antigen (PSMA) antibodies confirm PSMA expression in tumor-associated neovasculature. *Cancer Res.* 1999;59:3192–3198.
9. Rischpler C, Maurer T, Schwaiger M, Eiber M. Intense PSMA-expression using ^{68}Ga-PSMA PET/CT in a paravertebral schwannoma mimicking prostate cancer metastasis. *Eur J Nucl Med Mol Imaging.* 2016;43:193–194.
10. Demirci E, Sahin OE, Ocak M, Akovali B, Nematyazar J, Kabasakal L. Normal distribution pattern and physiological variants of ^{68}Ga-PSMA-11 PET/CT imaging. *Nucl Med Commun.* 2016;37:1169–1179.
11. Damle NA, Tripathi M, Chakraborty PS, et al. Unusual uptake of prostate specific tracer ^{68}Ga-PSMA-HBED-CC in a benign thyroid nodule. *Nucl Med Mol Imaging.* 2016;50:344–347.
12. Derlin T, Kreipe HH, Schumacher U, Soudah B. PSMA expression in tumor neovasculature endothelial cells of follicular thyroid adenoma as identified by molecular imaging using ^{68}Ga-PSMA ligand PET/CT. *Clin Nucl Med.* 2017;42:e173–e174.
13. Artigas C, Otte FX, Lemort M, van Velthoven R, Flamen P. Vertebral hemangioma mimicking bone metastasis in ^{68}Ga-PSMA ligand PET/CT. *Clin Nucl Med.* 2017;42:368–370.
14. Jochumsen MR, Vendelbo MH, Hoyer S, Bouchelouche K. Subcutaneous lobular capillary hemangioma on ^{68}Ga-PSMA PET/CT. *Clin Nucl Med.* 2017;42:e214–e215.
15. Krohn T, Verburg FA, Pufe T, et al. [^{68}Ga]PSMA-HBED uptake mimicking lymph node metastasis in coeliac ganglia: an important pitfall in clinical practice. *Eur J Nucl Med Mol Imaging.* 2015;42:210–214.
16. Beheshti M, Rezaee A, Langsteger W. ^{68}Ga-PSMA-HBED uptake on cervicothoracic (stellate) ganglia, a common pitfall on PET/CT. *Clin Nucl Med.* 2017;42:195–196.
17. Berger UV, Carter RE, McKee M, Coyle JT. N-acetylated alpha-linked acidic dipeptidase is expressed by non-myelinating Schwann cells in the peripheral nervous system. *J Neurocytol.* 1995;24:99–109.
18. Rauscher I, Maurer T, Steiger K, Schwaiger M, Eiber M. Image of the month: multifocal ^{68}Ga prostate-specific membrane antigen ligand uptake in the skeleton in a man with both prostate cancer and multiple myeloma. *Clin Nucl Med.* 2017;42:547–548.
19. Sheikhbahaei S, Afshar-Oromieh A, Eiber M, et al. Pearls and pitfalls in clinical interpretation of prostate-specific membrane antigen (PSMA)-targeted PET imaging. *Eur J Nucl Med Mol Imaging.* 2017;44:2117–2136.
20. Wang ZJ, Webb EM, Westphalen AC, Coakley FV, Yeh BM. Multi-detector row computed tomographic appearance of celiac ganglia. *J Comput Assist Tomogr.* 2010;34:343–347.
21. Levy M, Rajan E, Keeney G, Fletcher JG, Topazian M. Neural ganglia visualized by endoscopic ultrasound. *Am J Gastroenterol.* 2006;101:1787–1791.
22. Werner RA, Sheikhbahaei S, Jones KM, et al. Patterns of uptake of prostate-specific membrane antigen (PSMA)-targeted ^{18}F-DCFPyL in peripheral ganglia. *Ann Nucl Med.* 2017;31:696–702.
23. Jilg CA, Drendel V, Rischke HC, et al. Diagnostic accuracy of Ga-68-HBED-CC-PSMA-ligand-PET/CT before salvage lymph node dissection for recurrent prostate cancer. *Theranostics.* 2017;7:1770–1780.
24. Rauscher I, Maurer T, Beer AJ, et al. Value of ^{68}Ga-PSMA HBED-CC PET for the assessment of lymph node metastases in prostate cancer patients with biochemical recurrence: comparison with histopathology after salvage lymphadenectomy. *J Nucl Med.* 2016;57:1713–1719.